Clim Dyn (2018) 51:733–754
DOI 10.1007/s00382-017-3952-y

Evaluation of GCMs historical simulations of monthly and seasonal climatology over Bolivia

Azar M. Abadi[1] · **Robert Oglesby**[1] · **Clinton Rowe**[1] · **Rachindra Mawalagedara**[2]

Received: 16 June 2017 / Accepted: 2 October 2017 / Published online: 11 October 2017

Abstract Bolivia is a low-latitude, developing country at grave risk to the deleterious effects of human-induced climate changes. Due to the complexity of the topography in Bolivia, it is difficult to capture future impacts of the climate change on the regional scale with the coarse resolution of current GCMs. A robust strategy has been developed to dynamically downscale the GCM outputs to a more appropriate temporal and spatial resolution for impact studies. Prior to downscaling, however, evaluation of the GCMs used to provide large-scale forcing is a necessary step to ensure physically meaningful results from regional climate models. This study represents the first part of a broader project on evaluating climate change impacts over Bolivia. We examined precipitation, temperature, wind patterns and moisture transport to evaluate the performance of eight CMIP5 GCMs in simulating the continental and regional climate patterns. Phenomena including the seasonal and monthly positions of the intertropical convergence zone, South Atlantic convergence zone, Bolivian high, Chaco low and South American low-level jet, were analyzed. Our results confirm that, in general, all the GCMs do reasonably well in simulating the basic patterns of the variables with some discrepancies in magnitude across models, especially in the regional scale. Some models outperform the others for the variables and the region of our interest. Finally, the results of this research will help improve quantifying the uncertainty range of further regional downscaling outputs.

✉ Azar M. Abadi
azar@huskers.unl.edu

[1] Department of Earth and Atmospheric Sciences, University of Nebraska-Lincoln, Lincoln, NE, USA

[2] Department of Geological and Atmospheric Sciences, Iowa State University, Ames, IA, USA

1 Introduction

According to the Fifth Assessment Report (AR5) of the Intergovernmental Panel on Climate Change (IPCC 2013), the world's growing demand for food and biofuels has led to ongoing land cover change and increasing agricultural expansion in regions experiencing rapid development, including South America. Regional feedbacks of land surface-atmosphere interactions due to altering the natural ecosystems, along with the anthropogenic climate impacts owing to greenhouse gas emissions pose a significant threat to countries susceptible to water scarcity.

Bolivia is one of these vulnerable countries expected to face increases in temperature and dry spells, although of varying intensity and with different degrees of confidence in different regions of the country (Wheeler 2011). The country already appears to be suffering from global climate change impacts. Retreating glaciers in the Andes pose a threat to the regions with limited water resources over the Andes (Cook et al. 2016), and there is evidence of more frequent extreme events such as drought and flooding in regions such as Altiplano and La Plata basin in recent decades (Vicente-Serrano et al. 2014; Marengo et al. 2014; Ovando et al. 2016).

Local and regional land surface-atmosphere interaction can also exacerbate the anthropogenic global warming impacts. According to a Food and Agriculture Organization report (FAO 2010), among the countries in South America, Bolivia has the second highest rate of deforestation in its lowland tropical rainforests after Brazil. The lowlands in eastern Bolivia are also facing other stressors such as cattle ranching, agricultural expansion by indigenous colonies and urbanization. Studies show that the dry tropical forests of South America presently cover only approximately 40% of their former extension. The dry tropical forests of Chiquitano in southern Bolivia have also undergone extensive

deforestation, largely by conversion to croplands rather than to a tree plantation/crop mix as in Brazil (Sánchez-Azofeifa and Portillo-Quintero 2011; Salazar et al. 2015; Grau and Aide 2008). The negative impacts of combined anthropogenic and land use change can cause large-scale water imbalances, which in turn can result in significant feedbacks in the regional climate that may not be captured by coarse resolution global circulation models (GCM).

The complicated topography and high elevation of much of the country pose particular challenges, as these effects cannot be suitably resolved at the approximately 100 km spatial resolution of current global models. To assess any potential impacts of future climate change at a local scale, downscaling efforts are needed to describe these future climate changes better and to provide better input into the development of adaptation strategies. Even though regional climate models like the weather research and forecasting (WRF) model can depict local features more accurately, they are still dependent on their parent GCMs to simulate the larger scale climate patterns properly. Henceforth, selecting the proper GCM would be the first step for any downscaling job, and that motivates this study in advance of downscaling GCMs for Bolivia.

Section 2 provides an overview of the study area, the models, and observational datasets, and the general methodology for evaluating the climate models. In Sect. 3 we analyze the climate model depictions of continental and regional climate patterns of precipitation, air temperature, moisture budget and wind patterns in both lower and upper atmospheric levels. In Sect. 4 we discuss each models' ability to simulate the circulation patterns of the area, and in Sect. 5 we provide a summary of the study.

2 Data and methodology

2.1 Study area

Bolivia is a tropical country extending roughly from 10°S to 24°S in latitude and 56°W to 72°W in longitude (Fig. 1). Topography mainly dominates the climate in Bolivia in a way that according to Köppen climate classification,

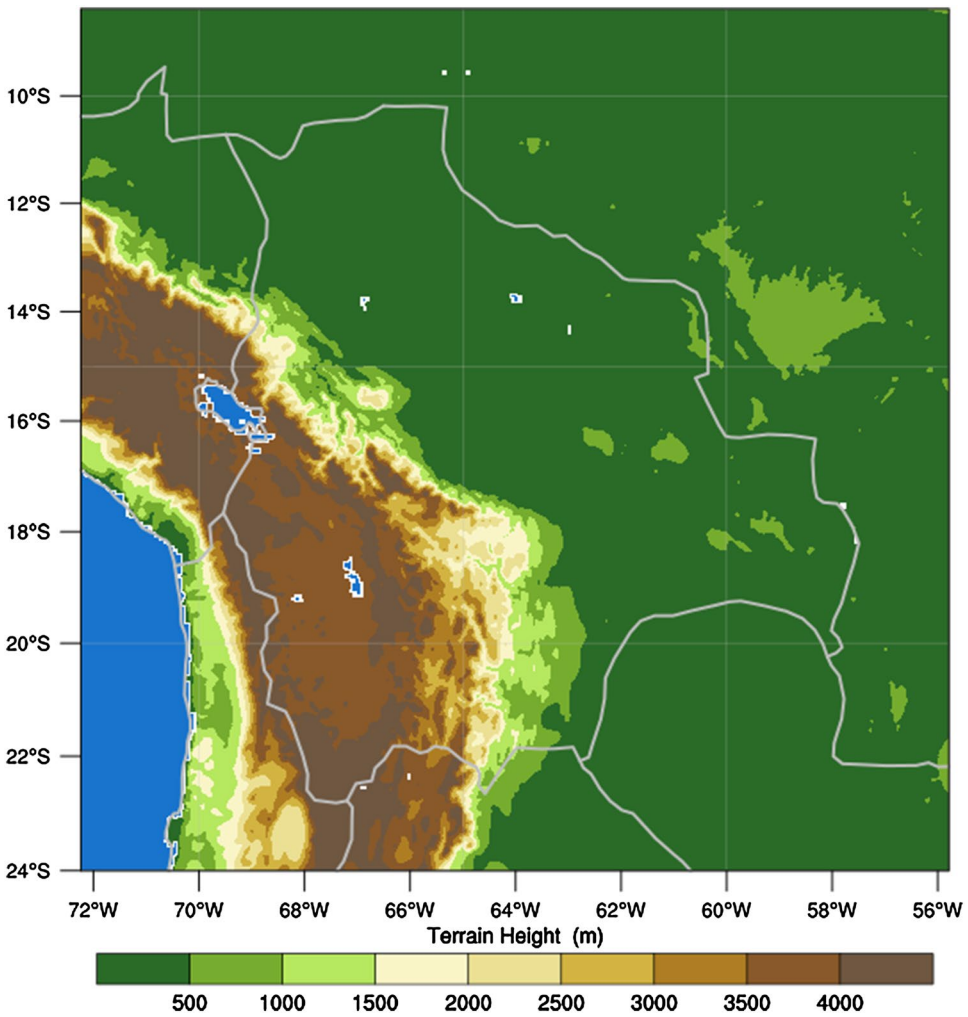

Fig. 1 Topography of Bolivia. Higher mountains of Andes lie to the west of the country with lowlands to the east. Units are in meters

lowlands in the northern and southeastern Bolivia have equatorial and dry tropical savanna types of climate, respectively. Higher valleys of the Cordillera Real, Cordillera Occidental and Altiplano in the middle are dominated by cold semi-arid to cold desert climate.

2.2 Models and observations

The coupled model intercomparison project phase 5 (CMIP5; Taylor et al. 2012) multi-model experiment provides climate data on which to examine climate predictability and assess climate change and variability. We evaluated one ensemble member for each of eight different CMIP5 GCMs from their historical runs. This subset of GCMs was selected based on their documented performances in generating realistic climate patterns in South America (Seiler et al. 2013a, b; Chou et al. 2011; Vera et al. 2006a, b; Jones and Carvalho 2013). Table 1 summarizes the eight chosen models, along with their spatial resolutions.

In this paper, we focus on the wet and dry months of January and July, respectively. The GCM outputs are verified using observational model reanalysis datasets of ERA-Interim for temperature, wind patterns and the moisture budget of the atmosphere, and the gauge-based product of global precipitation climatology project (GPCP) dataset for precipitation (summarized in Table 2) during 1979–2005.

The key question we address is the extent of each model's ability to reproduce the large-scale atmospheric features in terms of several statistical measures including mean, variability and pattern correlation. We first evaluate the seasonal climatology of these variables: precipitation, surface temperature, the lower level and upper level wind fields, and the moisture budget of the atmosphere. Finally, we summarize overall model performances in a matrix against all variable relative biases. All the statistical calculations have been done over two regions; one covering boundaries of Bolivia (8.4–24°S and 55.8–72.2°W as shown in Fig. 1) and the second one covering a larger area representing the continental-scale circulation (56°S–14°N and 31–84°W as shown in Fig. 3).

3 Results

3.1 Continental and regional climatology

While the Altiplano and western Cordillera receive limited amount of precipitation in wet months due to the complex topography of the Andes (Garreaud et al. 2003), the portion of Bolivia located to the east of Andes receives a large

Table 1 CMIP5 models evaluated, and their attributes

Model name	Spatial resolution	Center and references
CanESM2	2.8×2.8	Canadian Center for Climate Modeling and Analysis, Canada (Arora et al. 2011)
CCSM4	0.94×1.25	National Center for Atmospheric Research, United States (Gent et al. 2011)
CNRM-CM5	1.4×1.4	Centre National de Recherches Météorologiques/Centre Européen de Recherche et Formation Avancée en Calcul Scientifique, France (Voldoire et al. 2012)
HadGEM2-ES	1.24×1.8	Met Office Hadley Centre (additional HadGEM2-ES realizations contributed by Instituto Nacional de Pesquisas Espaciais), United Kingdom (Jones et al. 2011)
IPSL-CM5A-LR	1.875×3.75	Institute Pierre-Simon Laplace, France (Dufresne et al. 2013)
MIROC5	1.4×1.4	Atmosphere and Ocean Research Institute (The University of Tokyo), National Institute for Environmental Studies, and Japan Agency for Marine-Earth Science and Technology, Japan (Watanabe et al. 2010)
MIROC-ESM	2.8×2.8	Japan Agency for Marine-Earth Science and Technology, Atmosphere and Ocean Research Institute (The University of Tokyo), and National Institute for Environmental Studies, Japan (Watanabe et al. 2011)
MPI-ESM-LR	1.875×1.875	Max-Planck-Institut für Meteorologie (Max Planck Institute for Meteorology), Germany (Zanchettin et al. 2012)

Bold-italic models are the ones ultimately chosen for the purpose of downscaling

Table 2 Observational and reanalysis datasets

Observational dataset	Spatial resolution	Source and references
GPCP, precipitation	2.5 × 2.5	World Climate Research Program, International (Adler et al. 2003)
ERA-Interim, temperature	0.75 × 0.75	National Center for Meteorological Research, France (Dee et al. 2011)
ERA-Interim, wind components and specific humidity	0.75 × 0.75	National Center for Meteorological Research, France (Dee et al. 2011)

amount of precipitation in the summer months (DJF, with the peak in January) interacting with the South American Monsoon System (SAMS; Zhou and Lau 1998; Raia and Cavalcanti 2008; Marengo et al. 2012; Nogués-Paegle et al. 2002) and that is why we are mainly focused on the eastern side of the Andes. The significant seasonal change in the wind regime over South American tropics and subtropics as part of this monsoon system is responsible for the seasonal variability of rainfall (Wanzeler da Costa and Satyamurty 2016) which brings little to no precipitation to Bolivia in the austral winter (JJA, with July as the driest month).

The circulation around the subtropical high pressure in Atlantic Ocean (South Atlantic Subtropical High; SASH) drives warm and moist air via the trade winds to the north-eastern part of South America (Arraut and Satyamurty 2009; Marengo et al. 2012), leading to precipitation in most of the Amazon basin, including Bolivia's northern lowlands (Fig. 2). Closer to the eastern Andes, the near surface wind is channeled between the tropics and mid-latitudes into the South American Low Level Jet (SALLJ: Campetella and Vera 2002; Liebmann et al. 2004; Marengo et al. 2012). This low-level jet reaches its maximum at 1–2 km above the surface, with the strongest winds observed over Santa Cruz de la Sierra in Bolivia (Vera et al. 2006b). The SALLJ is a characteristic of the warm monsoonal season and plays an important role in transporting moisture from the tropics to the higher latitudes, bringing convection and rainfall at the exit region of the jet (Haylock et al. 2006). Several studies have shown that the dynamical modification to the mean circulation introduced by the Andes sustains the maximum wind over Bolivia all year round (Vera et al. 2006a, b; Byerle and Peagle 2002).

The latent heat released from the Amazonian precipitation during the wet months and the seasonal heating of Altiplano combine to give rise to an upper level anticyclone known as the Bolivian high (Lenters and Cook 1997, 1999; Zhou and Lau 1998). At the surface, a thermally driven low pressure system (i.e., the Chaco low) strengthens over southeastern Bolivia and northern Paraguay which, along with the strengthened low-level jet, increases downstream moisture advection from the Amazon basin towards La Plata basin (Marengo et al. 2004; Salio et al. 2007; Liebmann and Mechoso 2011; Vera et al. 2006b; Berbery and Barros 2002).

Moisture-laden counterclockwise circulation around the Atlantic subtropical high pressure accompanied by the Chaco low's clockwise circulation, creates convergent winds and a northwest-southeast oriented region of clouds and precipitation known as South Atlantic convergence zone (SACZ; Carvalho et al. 2011; Marengo et al. 2012; Liebmann et al. 2004). In July (austral winter), this thermal low, the Bolivian high and the SACZ all dissipate. This results in reduced moisture transport from the Amazon basin to the Bolivian lowlands, causing less rainfall in the interior of the continent. As the ITCZ (intertropical convergence zone) travels northward and westerly winds replace easterlies in the upper troposphere over Bolivia, moisture transport is inhibited from the lowlands to the Andes, causing precipitation to be limited to the northern part of the country (Garreaud et al. 2003). Figure 2 shows a schematic illustration of atmospheric circulations during the austral summer (January).

3.2 Precipitation climatology

Figure 3 compares the climatology of the modeled and observed precipitation for January and July, respectively, for the period of 1979–2005. All the models simulate the large-scale spatial patterns of precipitation fairly well, with higher precipitation in the Amazon region during January, and mainly drier conditions in July over central parts of the

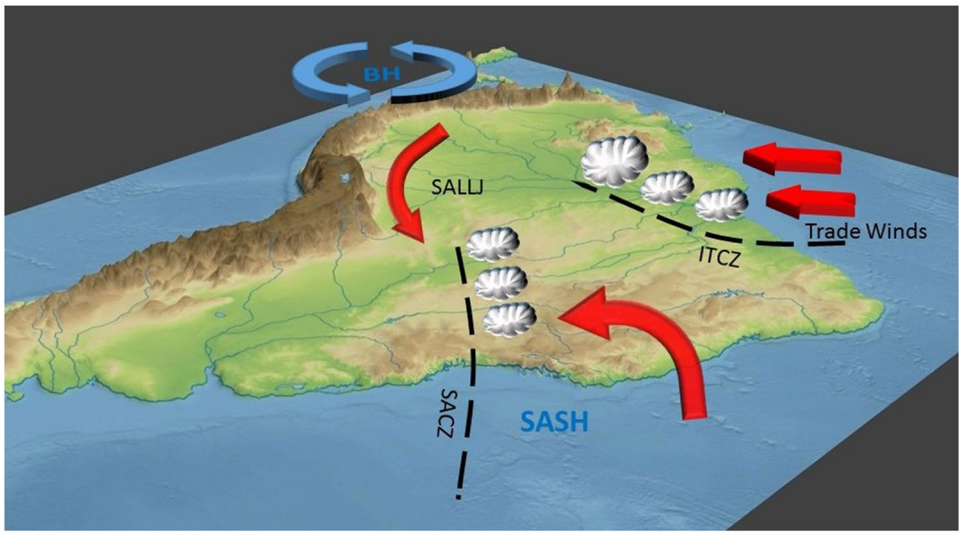

Fig. 2 Schematic of the large-scale circulation features that affect Bolivia's regional climate during the wet months. SASH represents South Atlantic Subtropical High. Red straight arrows show the trade winds blowing to the continent from northeast. The narrow red curved arrow depicts low-level jet, while the thick red arrow shows the northern branch of SASH. The counter-clockwise circulation over the Andes pictures the Bolivian high and dashed black lines illustrate intertropical convergence zone (ITCZ) and South Atlantic convergence zone (SACZ)

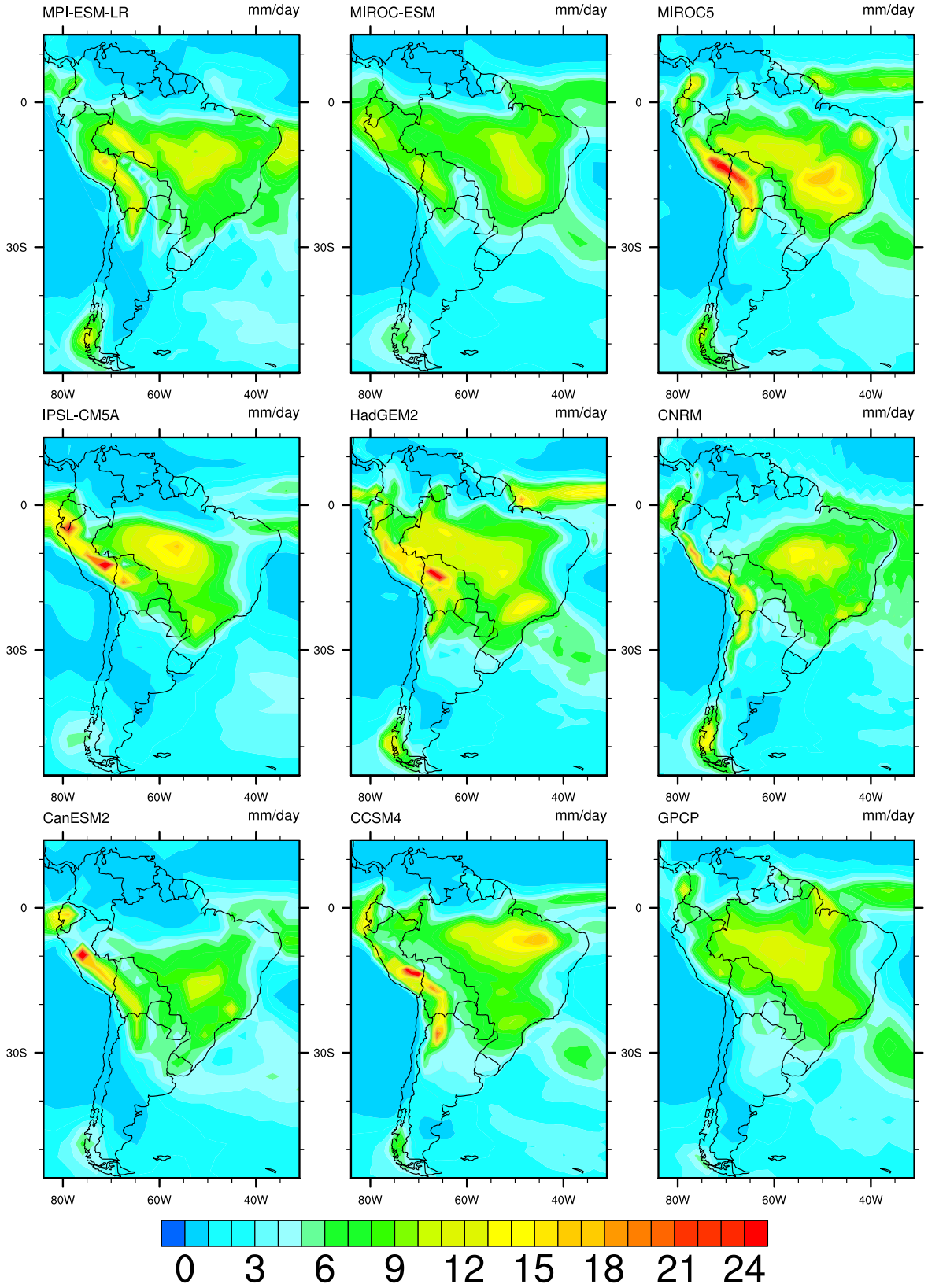

Fig. 3 Precipitation climatology (1979–2005) for CMIP5 models and GPCP dataset **a** January and **b** July. The model data are shown at their original spatial resolution. Units are in mm/day

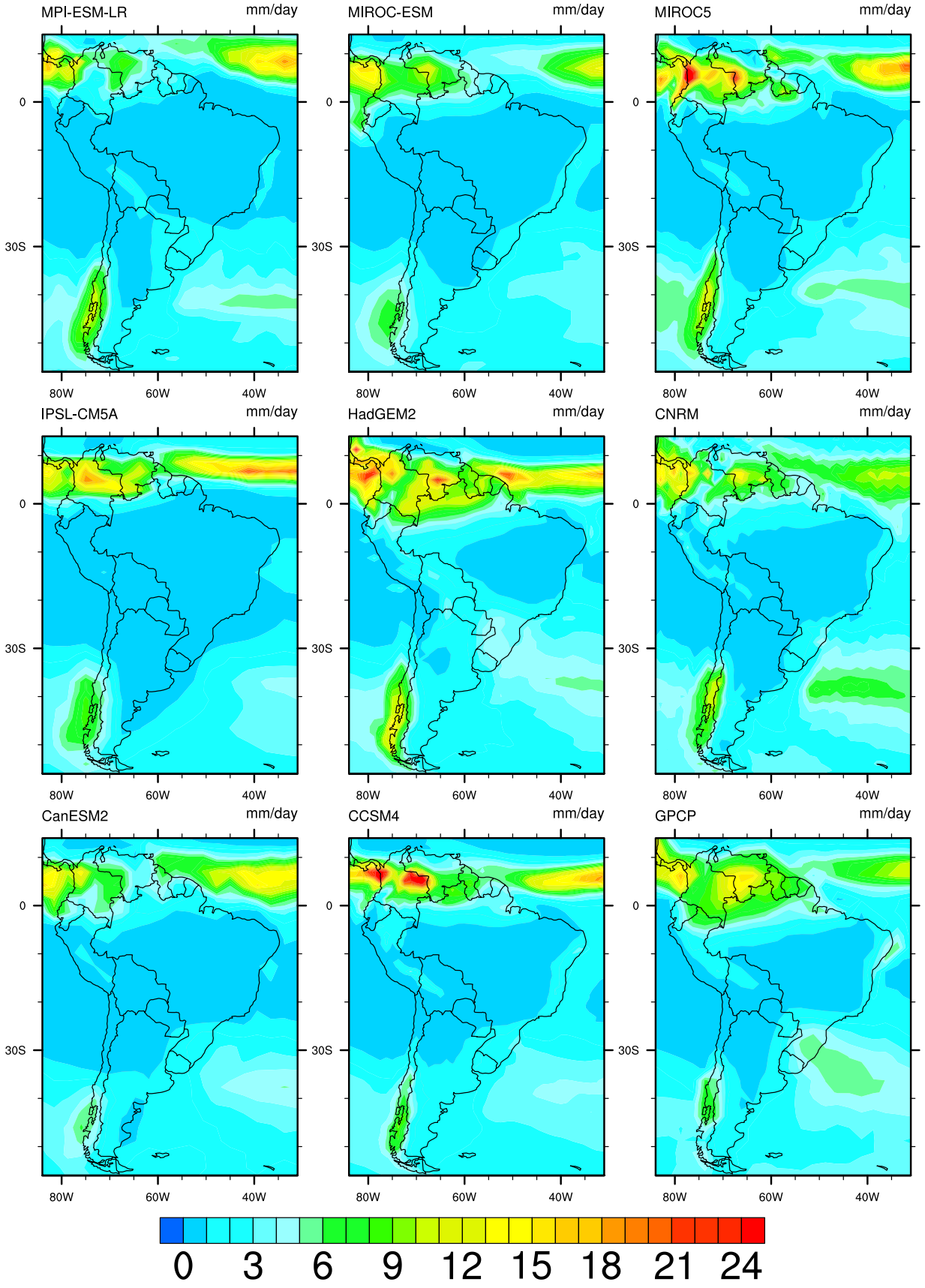

Fig. 3 (continued)

continent (Zhou and Lau 2001; Vera et al. 2002; Gan et al. 2004; Grimm 2011; Blacutt et al. 2015). Though the GCMs are broadly similar at the largest scales, there are substantive differences at regional scales. In the wet season most of the models get the ITCZ and SACZ's geographical locations and extensions close to observations (the exceptions being CanESM2, MPI-ESM-LR and CNRM-CM5), though the intensity of the precipitation differs between models. During the austral winter (Fig. 3) which is the dry season for most of the study area, the regions of maximum precipitation are confined to the northern parts of the continent, associated with the northward shift of ITCZ, and southeastern South America, reflecting the role of synoptic phenomena and frontal passages (Raia and Cavalcanti 2008; Vera et al. 2002).

The main difference among the models is in the simulated intensity of the precipitation. All of the models overestimate precipitation to some extent over the Andes during the wet months (as shown in Table 3; Fig. 3), a common behavior of the models over elevated terrains which is likely due to deficiencies in capturing the actual extent of the real topography. This may also be in part due to the precipitation underestimation in gridded observations, especially over mountainous regions where the reliability of the gridded observational datasets is questionable. According to the observations, higher rainfall occurs in the northern lowlands of Amazonia with lower amounts of rainfall at higher elevations. Table 3 represents the spatially averaged biases in modeled precipitation divided by the observation (% of observed mean).

Figure 4 charts the seasonal cycle of precipitation in Bolivia. All of the eight GCMs reproduce the seasonal pattern of precipitation very well in terms of the timing of the maximum and minimum precipitation. However, some discrepancies occurs among models for the magnitude of precipitation. All of the models except MIROC-ESM overestimate the amount of precipitation to some degree during the wet months, but simulate the precipitation in drier months closer to that observed except the HadGEM2-ES. Figure 5 shows the frequency distribution of rainfall over Bolivia in the month of January. As it is evident in this figure, some models, including MIROC5, IPSL-CM5A-LR and HadGEM2-ES, show some skewness towards a higher amount of precipitation compared to observations, in agreement with Figs. 3 and 4. That shows the abovementioned models underestimate the frequency of lighter precipitation and overestimate moderate to heavier precipitation events (Solman et al. 2013).

Table 3 Mean biases percentage (bias/observation) for CMIP5 simulated precipitation relative to GPCP observations in months of January and July averaged over Bolivia and a larger region representing the continent

Model	Bolivia		Continent	
	Jan	Jul	Jan	Jul
MPI-ESM-LR	10.51	−12.89	−7.22	−68.44
MIROC-ESM	−7.93	−48.56	−4.96	−57.87
MIROC5	35.65	−45.57	9.72	−52.38
IPSL-CM5A-LR	17.53	−82.51	5.06	−80.66
HadGEM2-ES	40.42	159.26	18.91	34.00
CNRM-CM5	−2.15	−28.84	−15.05	−43.83
CanESM2	−9.14	−58.29	−20.38	−53.65
CCSM4	3.47	−44.67	10.29	−48.92

3.3 Surface air temperature

Figure 6 depicts the January and July temperature climatology for the GCMs and observations over the period 1979–2005. Following the terrain, lower temperatures are observed in the higher elevations (Cordillera Real, Cordillera Occidental and Altiplano), with higher temperatures in the lowlands (Solman et al. 2013). During the warm season, all the models simulate the basic large-scale spatial pattern of the temperature—warmer over the lowlands and cooler over the mountains. In July, models follow the observation with highest temperatures over the Amazon region with a well-defined North–South temperature gradient.

In January there is also a local temperature maximum in Chaco region (southeastern Bolivia and northern Paraguay) due to the presence of the thermal Chaco low which is replaced by cold air in the winter (Garreaud et al. 2009). There are warm biases over the Andes in most of the models, especially in July, likely due to the coarse resolution of the GCMs that cannot resolve sufficiently the vertical extent of the mountain ranges.

The difference between the models and observations in some areas exceeds 2–3 °C, and is most evident in MIROC-ESM and CanESM2 overestimating the temperature in January over Andes and northern part of the continent, respectively. There are also warm biases along the western coast of the continent from Northern Chile to northern Peru in almost all of the GCMs (the one exception being IPSL-CM5A-LR) which shows that the models likely are underestimating the intensity of the cold Peru/Humboldt current (Penven 2005). Considering the fact that sea surface temperature exerts a significant control on precipitation in regions adjacent to the ocean, this warm bias then helps to explain the modeled wet biases over the Andes. Table 4 summarizes the mean biases of the temperature averaged over Bolivia and Continent regions. By comparing the values between the two regions, it is evident that reducing the size of the region increases the averaged error due to improper physics of the GCMs at a regional scale. This is further evidence that motivates the authors for downscaling GCMs to study the impacts at a local scale. MPI-ESM-LR, HadGEM2-ES and CNRM-CM5

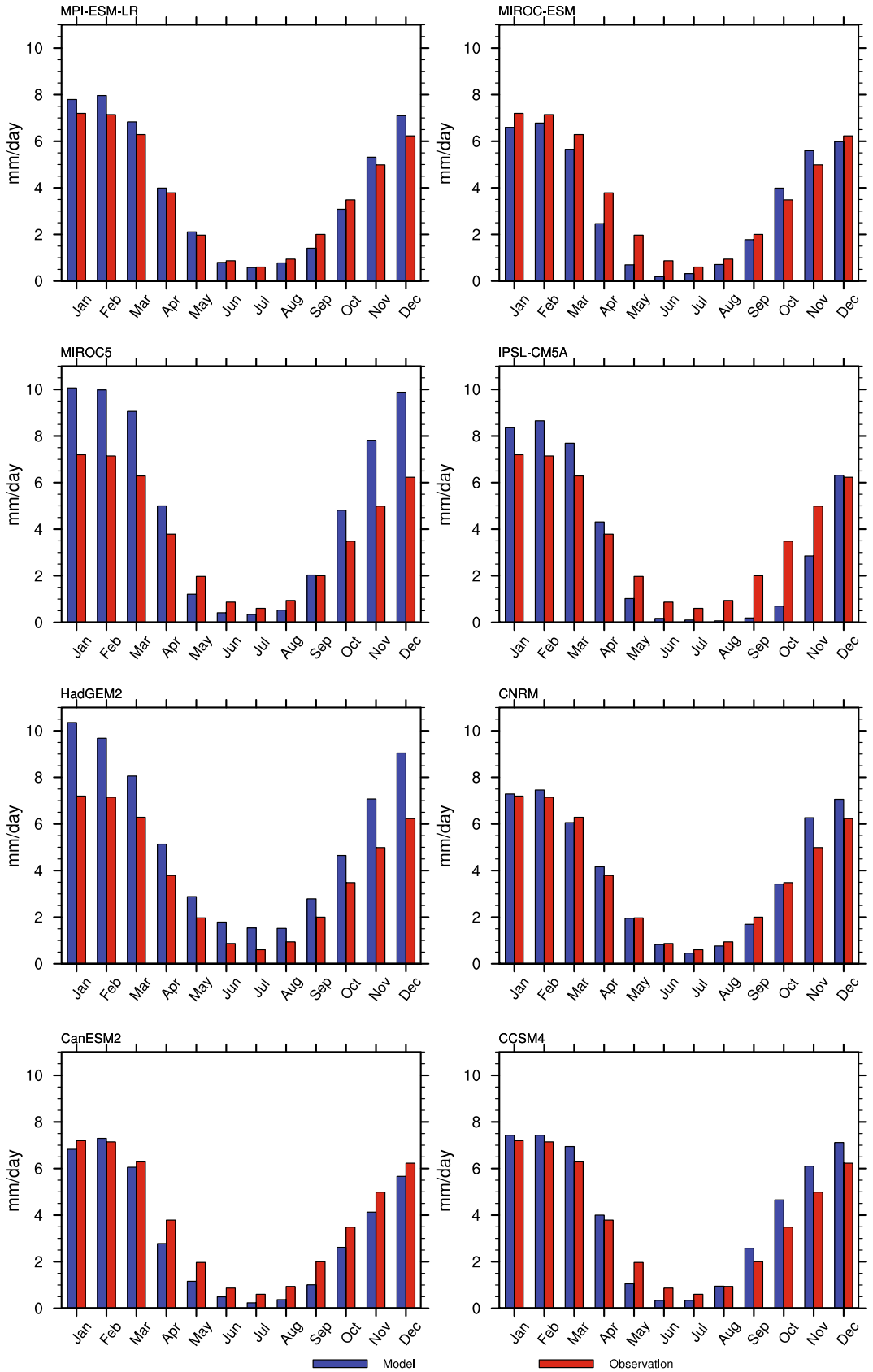

Fig. 4 Observed and simulated seasonal cycle of monthly precipitation averaged over Bolivia (in mm/day)

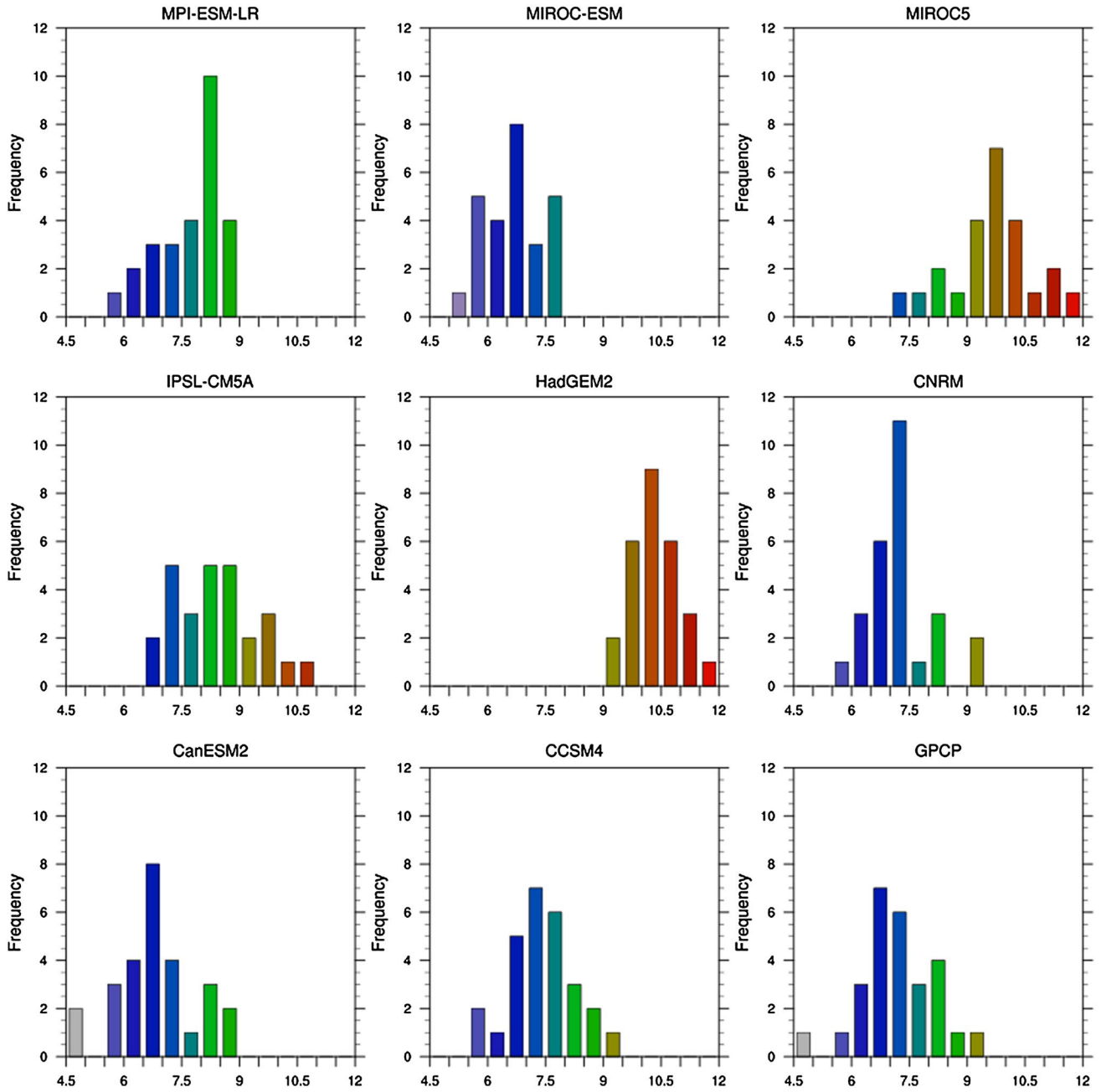

Fig. 5 Frequency distribution of monthly precipitation for January from 1979 to 2005, with higher values for precipitation in red and lower values in blue (in mm/day)

tend to underestimate the temperature over Bolivia while the other models overestimate it.

The annual cycle of the temperature is shown in Fig. 7. Most of the models follow the observed annual cycle of temperature reaching a maximum in December–January and a minimum in July. However, the amplitudes vary among models with some mainly underestimating the surface temperature including HadGEM2-ES, CNRM-CM5 and MPI-ESM-LR while the rest of them overestimate the temperature (Table 4).

3.4 Upper and lower level atmospheric circulation patterns

Figures 8 and 9 show the lower (850 hPa) and upper (200 hPa) level atmospheric mean circulation patterns for January and July, respectively. In January (Fig. 8a), trade

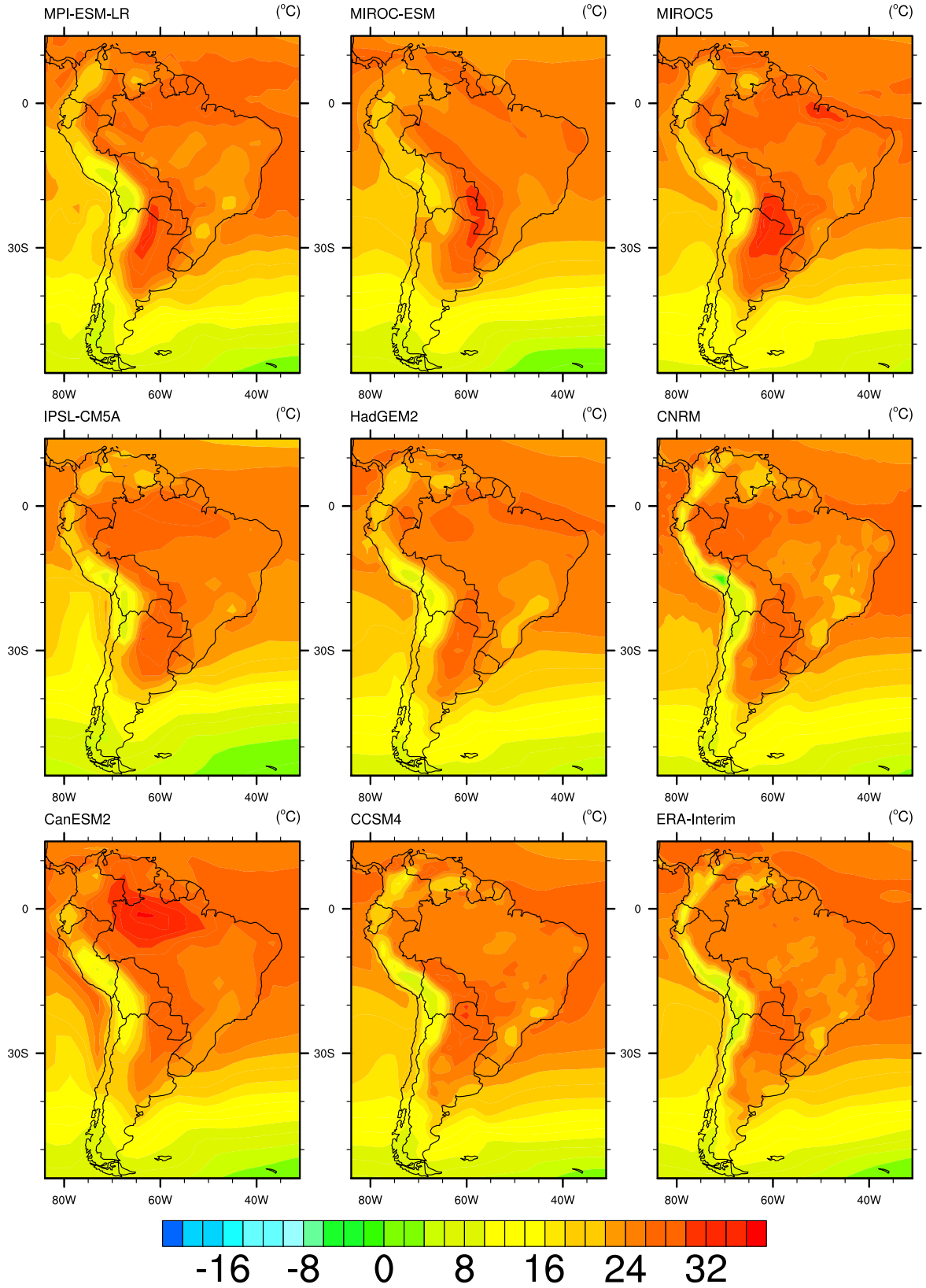

Fig. 6 Surface temperature climatology (1979–2005) for CMIP5 models and ERA-Interim dataset for January (**a**) and July (**b**). The model data are shown at their original spatial resolution. Units are in °C

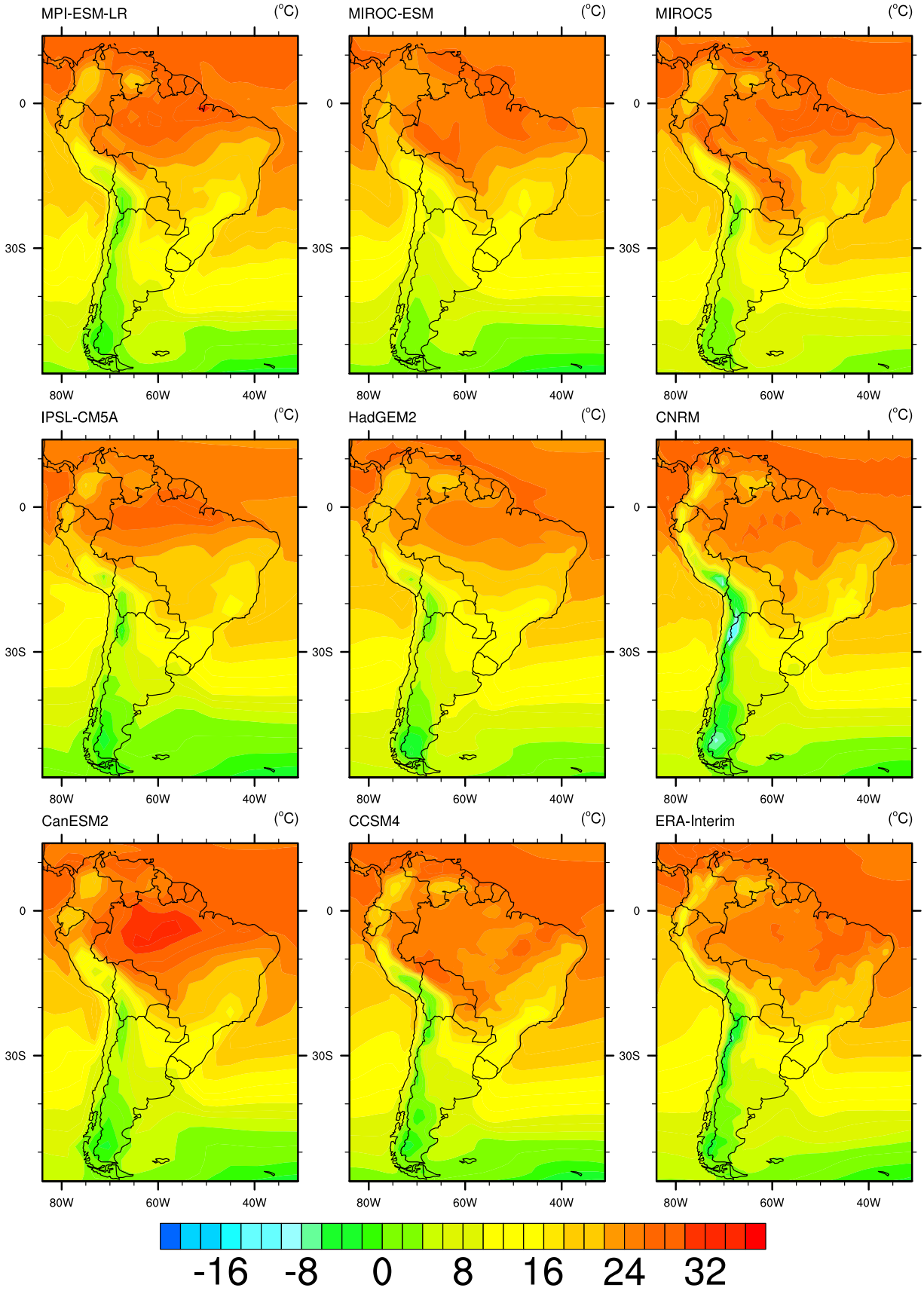

Fig. 6 (continued)

Table 4 January and July biases in CMIP5 simulated temperature relative to ERA-Interim observations averaged over Bolivia and a larger region representing the continent

Model	Bolivia		Continent	
	Jan	Jul	Jan	Jul
MPI-ESM-LR	−0.84	−1.82	−0.15	0.06
MIROC-ESM	1.80	1.03	−0.53	−0.23
MIROC5	1.25	2.21	0.45	1.10
IPSL-CM5A-LR	0.55	−0.93	−1.28	−1.38
HadGEM2-ES	−0.51	−2.33	−0.15	−0.54
CNRM-CM5	−0.35	−1.42	0.03	−0.38
CanESM2	1.16	1.61	0.51	0.30
CCSM4	0.62	1.62	0.05	0.21

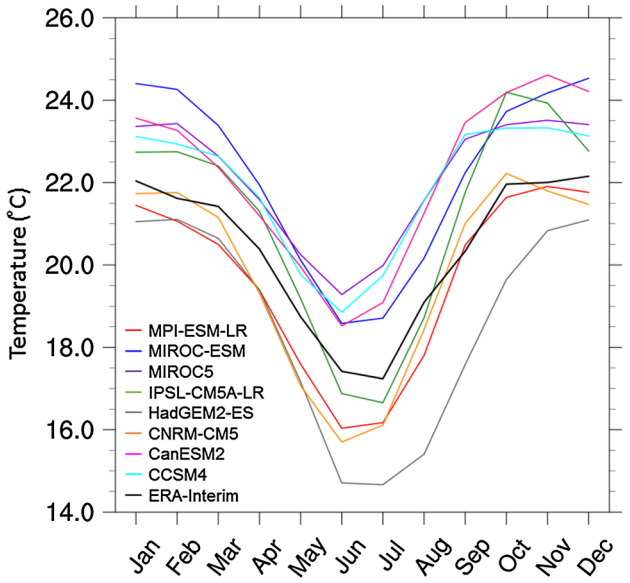

Fig. 7 Observed and simulated seasonal cycle of monthly temperature averaged over Bolivia (in °C)

winds that blow onto the continent from the northeast are channeled by the Andes, creating the SALLJ. As described earlier, the SALLJ carries tropical warm and moist air into the central part of the continent, which then fuels deep convective precipitation. In austral winter the ITCZ migrates north, pushing the trade winds northward as well, which leads to less moisture advection onto the continent (Fig. 8b; Zhou and Lau 2001; Liebmann et al. 2004; Marengo et al. 2004, 2012). All the GCMs capture this wind pattern, with some discrepancies among models in the magnitude of trade winds. The greater the magnitude of the simulated winds, the more moisture they will carry further south, leaving Amazonia with less available water vapor. That might help explain some of the dry biases over the Amazon basin and wet biases further south toward the Andes during the summer in models including CanESM2, CNRM-CM5, IPSL-CM5A-LR and MPI-ESM-LR (bias maps not shown).

Figure 9 summarizes the observed and simulated features of the upper level circulation in South America including the effects of the Bolivian high. Excluding CanESM2 and IPSL-CM5A-LR, the remaining models reproduce the anticyclone's location and intensity close to that in the reanalysis dataset. The position and the intensity of the upper level Bolivian high combined with favorable conditions for convective development in the lower level atmosphere (sufficient water vapor) play an important role (Garreaud et al. 2003) in the heavy convective precipitation that takes place during summer over the Altiplano. Insel et al. (2013) showed that the upper level easterlies, resulting from the northern branch of Bolivian high, not only can provide basic horizontal moisture advection, but also can modulate and strengthen upslope circulations, leading to even more moisture transport into the Altiplano. Heating of the elevated terrain also creates a regional up-slope circulation focused on the eastern cordillera slopes, which helps transport moisture to the Bolivian highlands. In winter (Fig. 9b), westerlies and a stronger jet stream prevail in the upper levels, hindering moisture transport from the lowlands to higher valleys, with the impact on precipitation noticeable in Fig. 3.

3.5 Moisture budget of the atmosphere

To understand the above effects better, we investigated the moisture budget of the atmosphere by examining the climatology of moisture transport over the continent, especially Bolivia, as well as the vertically integrated moisture flux convergence for the period of 1979–2005 with a continued focus on January and July. Newman et al. (2012), ignoring relatively small interannual variations of precipitable water, concluded that the vertically integrated moisture flux convergence can be used to estimate the moisture budget, therefore the imbalance between precipitation and evaporation. In the same research, they also studied the contribution of transient and low frequency eddies, as well as time-mean circulation, to the total moisture transport and summarized the mean moisture transport as

$$\bar{Q} = \bar{Q}^m + \bar{Q}^{LF} + \bar{Q}^s$$

where the right hand side terms represent transport by the time-mean flow, low frequency anomalies and synoptic anomalies, respectively. Since their results show clearly that the moisture transport is dominated by time-mean flow in the lower latitudes, we have focused on the mean term in the equation, for the present study. For analysis of the moisture field climatology, horizontal wind components and specific humidity fields from the surface to 300-hPa were extracted from GCMs and ERA-Interim reanalysis datasets for the period of 1979–2005.

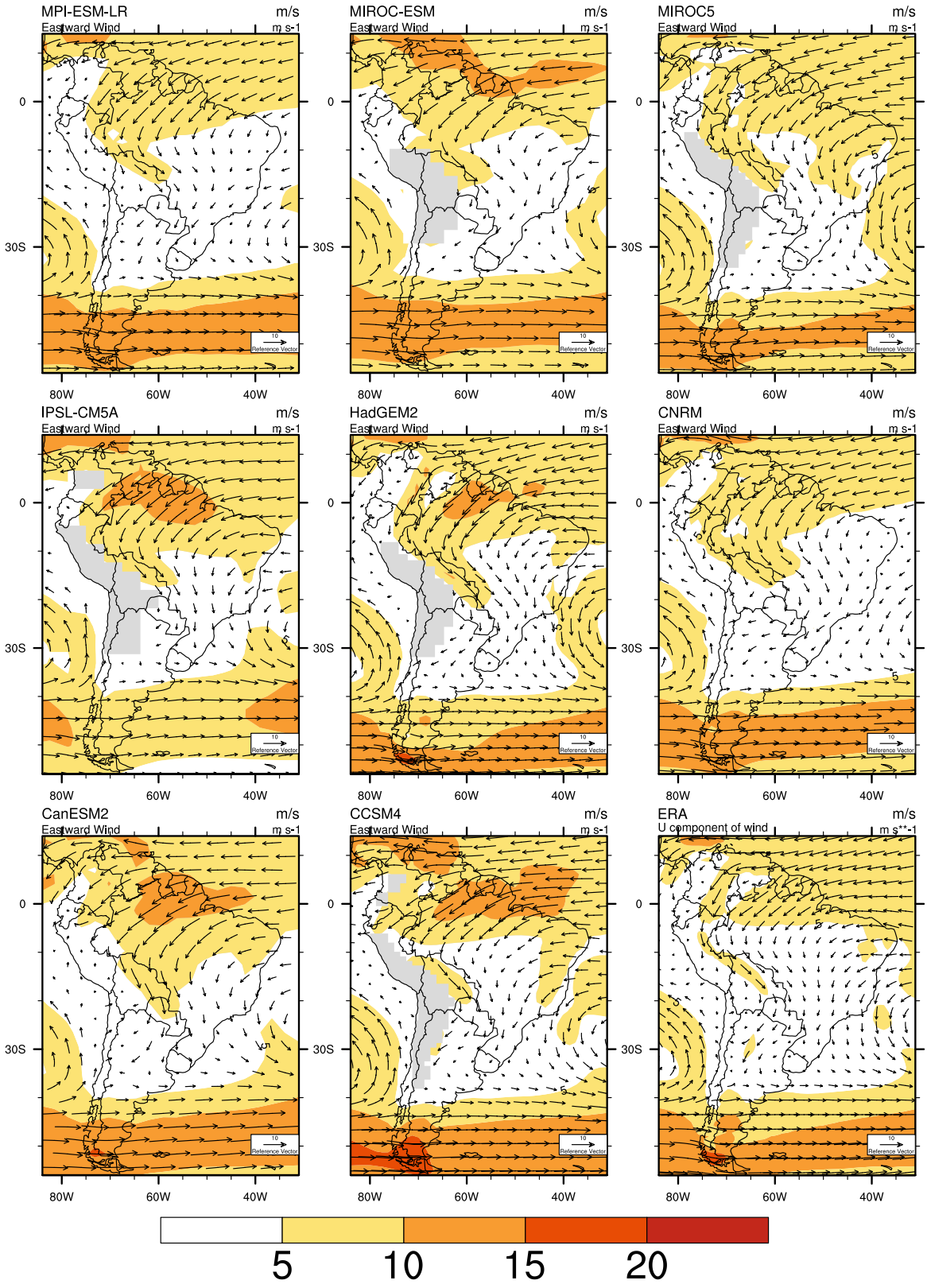

Fig. 8 Wind vector climatology (1979–2005) at 850 hPa for CMIP5 models and ERA-Interim in January (**a**) and July (**b**). The model data are shown at their original spatial resolution

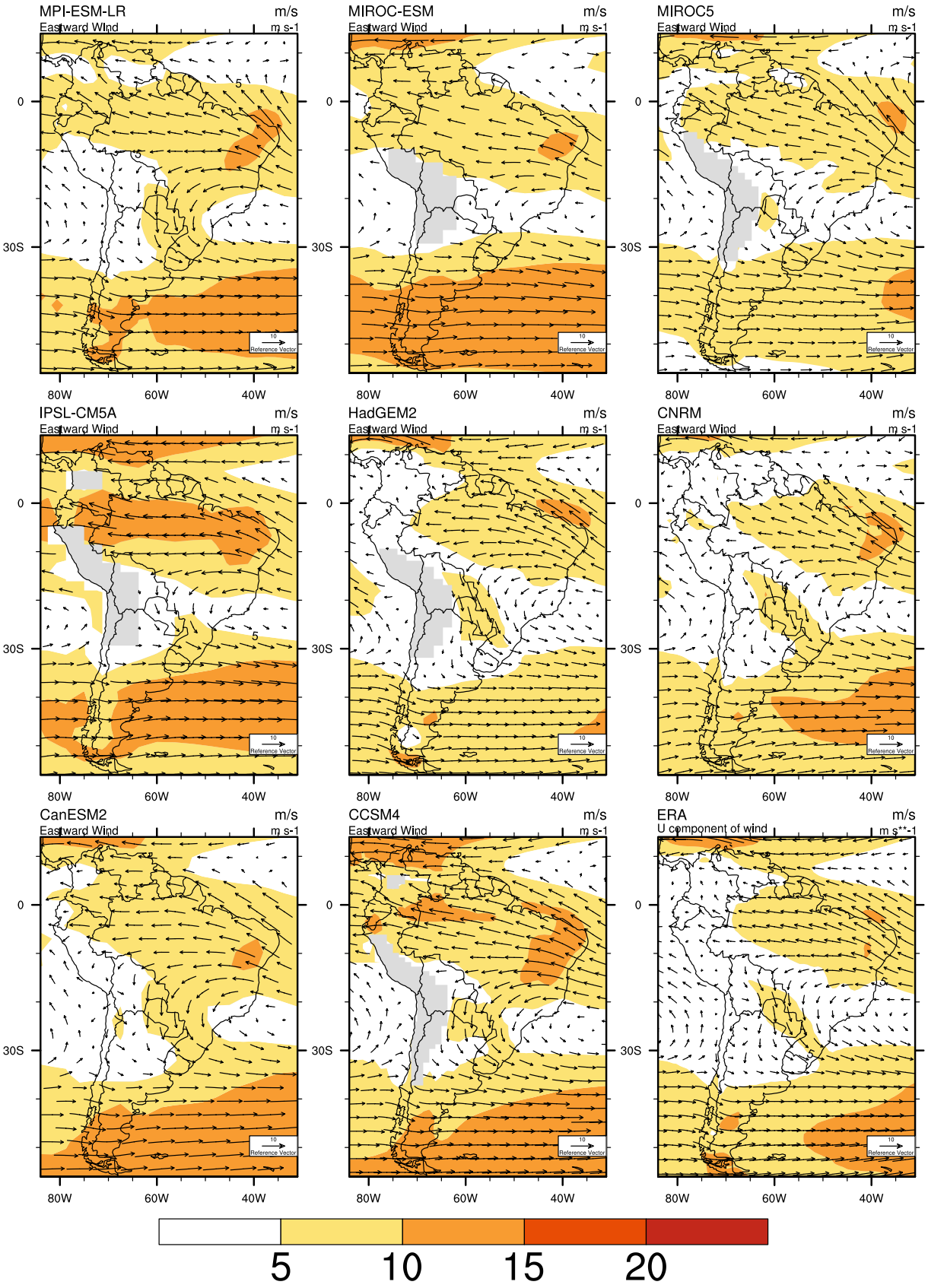

Fig. 8 (continued)

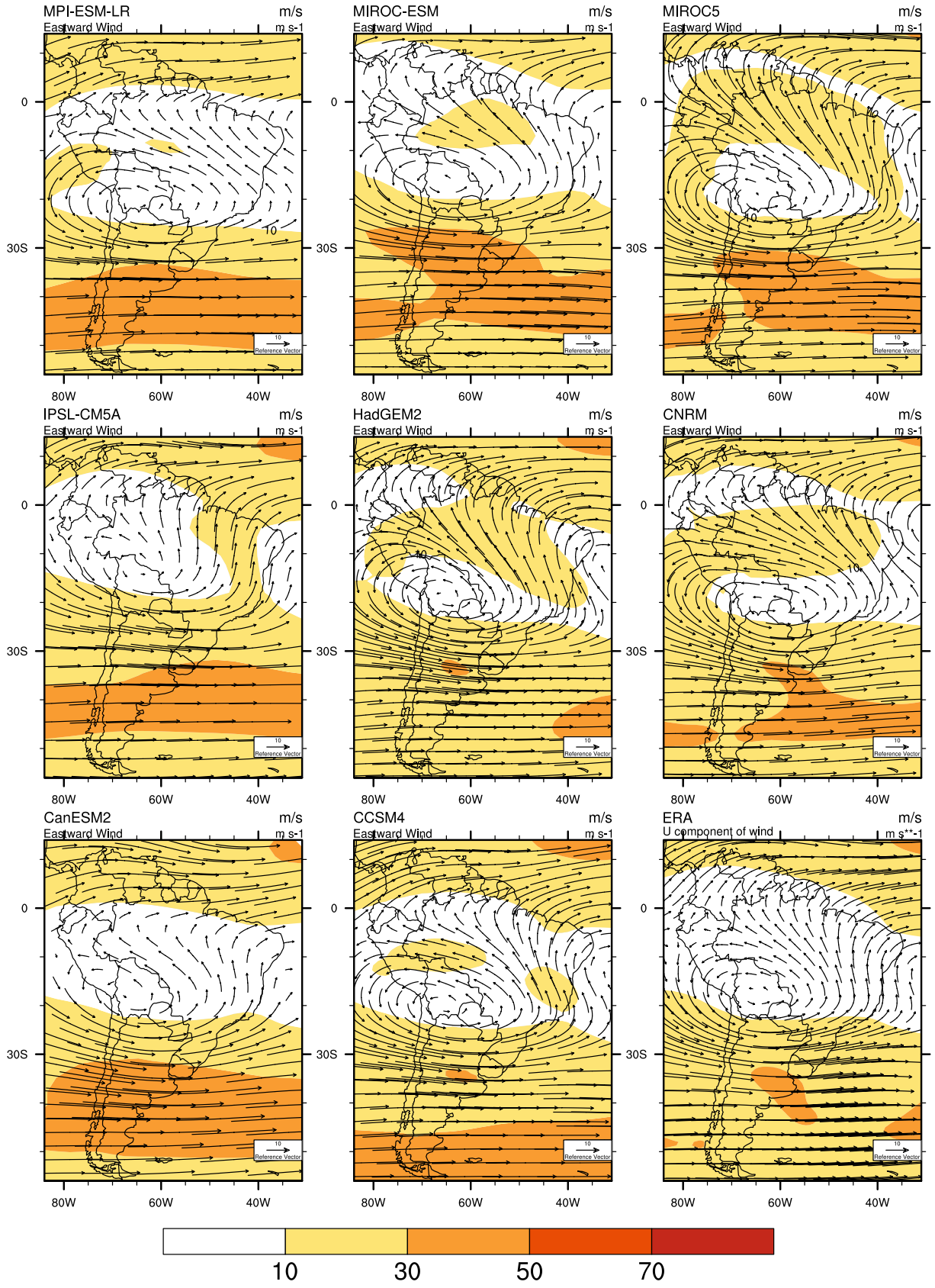

Fig. 9 Wind vector climatology (1979–2005) at 200 hPa for CMIP5 models and ERA-Interim in January (**a**) and July (**b**). The model data are shown at their original spatial resolution

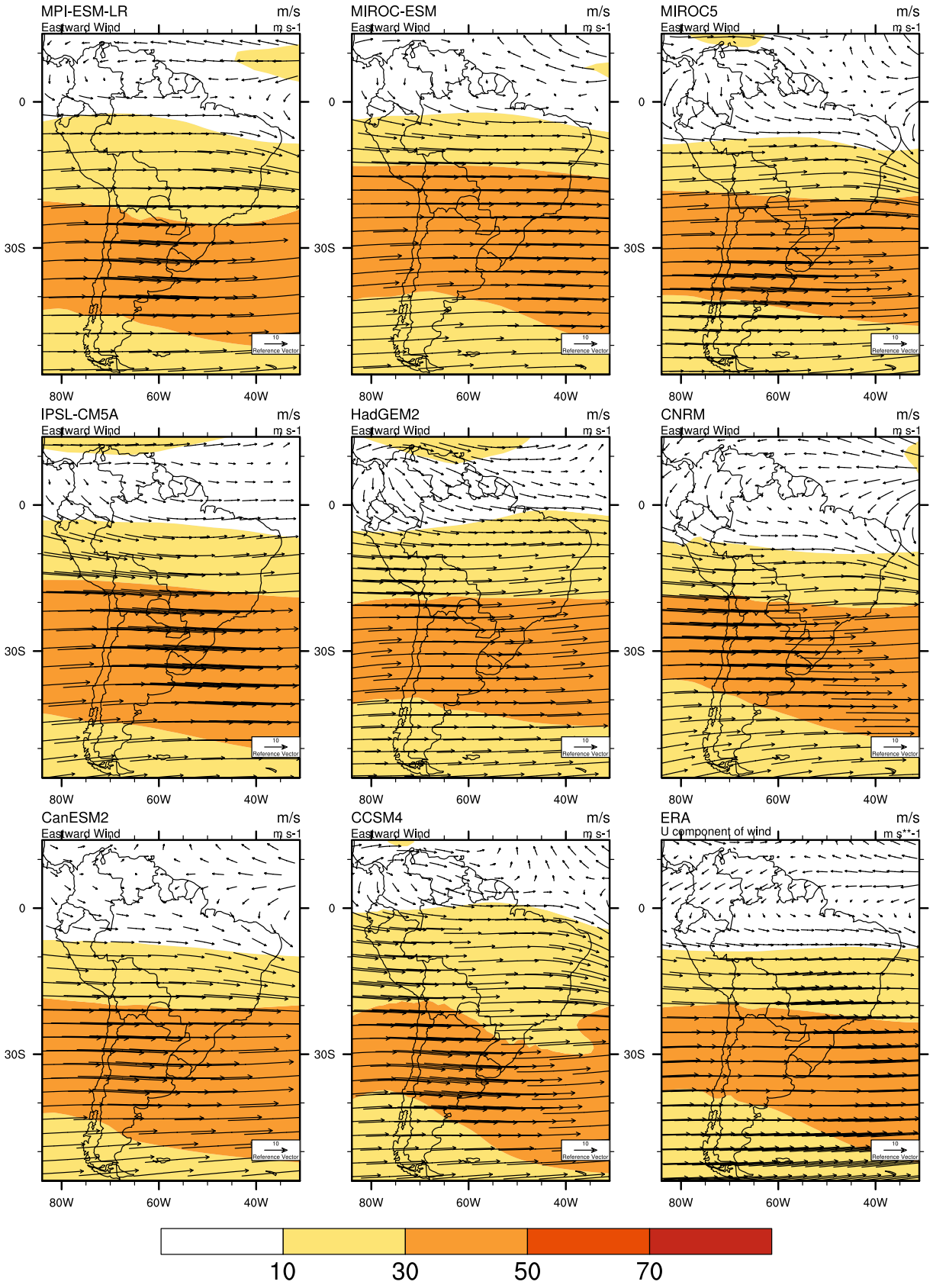

Fig. 9 (continued)

Figure 10 compares the climatology of CMIP5 models' vertically integrated moisture fluxes (vectors) and associated convergences (contours) to the observational estimates from ERA-Interim for the months of January and July. The mean moisture flow over Amazonia during the warm season is dominated by the interhemispheric northeasterly trade winds which, as described above, is also associated with convergence over the Andes. This transport is then deflected by the Andes and intensified by SALLJ so the moisture can reach La Plata basin (Marengo et al. 2004; Soares and Marengo 2009). In January, almost all the models compare well with the reanalysis in the position and the intensity of the moisture transport by trade winds and the subtropical high, with the convergence mainly over Amazonia and the Andes, where the maximum precipitation is observed in ITCZ and SACZ, respectively. These results are consistent with other studies in South America including Carvalho et al. (2011), Wanzeler da Costa and Satyamurty (2016), Raia and Cavalcanti (2008), Satyamurty et al. (2013) and Berbery and Barros (2002). The models also simulate the strong divergence in the tropics and east coast of Brazil where the Brazilian plateau blocks the low-level circulation. Comparing the spatial patterns of the models and the observations, it is clear that some models have deficiencies in simulating the strength of the ITCZ, including MPI-ESM-LR, CNRM-CM5, IPSL-CM5A-LR and CanESM2, which was also evident in the precipitation underestimation in the same region (Fig. 3). The strong moisture convergences represent the places where precipitation exceeds evaporation. These regions act as a sink of atmospheric moisture and overlap the regions with the maximum precipitation (Fig. 3). On the other hand, places with strong divergence serve as moisture sources to the atmosphere, with evaporation exceeding the precipitation (Trenberth et al. 2011), which is the case over Amazonia in the austral winter. There is a reasonable agreement on the locations and intensities of precipitation and convergence among all the GCMs.

In austral winter, with the subtropical high traveling further north and west, southeasterly winds replace northeasterly trade winds in the northeastern part of the continent. This southeasterly flow leaves Amazonia drier with less moisture transport (Fig. 10b).

4 Discussion

We evaluated the credibility of eight CMIP5 models in terms of simulating the large scale circulation over South America, with a particular focus on Bolivia and surrounding regions. Our emphasis is on the implications of these large-scale circulation features for local temperatures and precipitation at the surface. We presented the mean spatial distribution of precipitation, surface temperature, upper and lower level wind components, and the moisture budget of the atmosphere. No one standard performance tool has been found to apply for all types of evaluations (Sheffield et al. 2013; Gleckler et al. 2008). For the purpose of this study, therefore, we have focused on comparative assessments including spatial correlations (Pearson correlation coefficient) and standard deviations in the form of Taylor diagram and normalized biases in the form of a matrix of climate model credibility (Rupp et al. 2013).

A Taylor diagram (Fig. 11) compares the spatial correlation (shown with regard to the azimuthal angle) and the normalized standard deviation of the models' simulated January mean precipitations and temperatures versus observation (radial distance from the origin) over Bolivia. We choose January since it represents the rainy season for most of our region of interest. Most of the models very closely reproduce the spatial distribution of precipitation and temperature over Bolivia, as the correlation is above 0.88 for all the models for both variables. However the models are more successful in simulating the spatial distribution of temperature than that of precipitation (Oglesby et al. 2016), with higher correlation values (≥ 0.98).

The normalized standard deviation is the standard deviation of the model data normalized by the standard deviation of the observations, such that the closer a model is to the observation point (ref point), the lower the RMS error would be (Gleckler et al. 2008). The January diagram shows that more than half of the models underestimate the spatial variability of both precipitation and surface temperature over the larger region, and the remaining models overestimate it. Among these models, MPI-ESM-LR, IPSL-CM5A-LR, CNRM-CM5 and MIROC5 stand out as they have relatively high spatial correlations and lie closer to the Ref point that indicates perfect agreement with observations. In July (not shown), we find high correlations on temperature among the aforementioned outstanding models, with lower agreements on precipitation among models, which is not surprising considering the low amount of precipitation during this dry season.

Finally, Fig. 12 summarizes the model biases for precipitation, temperature and moisture convergence with respect to the observations over the two regions, one focused on Bolivia and the other a broader region covering most of central South America so as to capture the larger scale. The biases for each variable are normalized, as

$$Score = \frac{B_i - B_{min}}{B_{max} - B_{min}}$$

where B_i is the bias for model i for a certain variable and B_{min} and B_{max} are the minimum and maximum biases, respectively, across all the models. Thus, a model gains a score between 0 and 1 (Fig. 12) with a score closer to 0 (1)

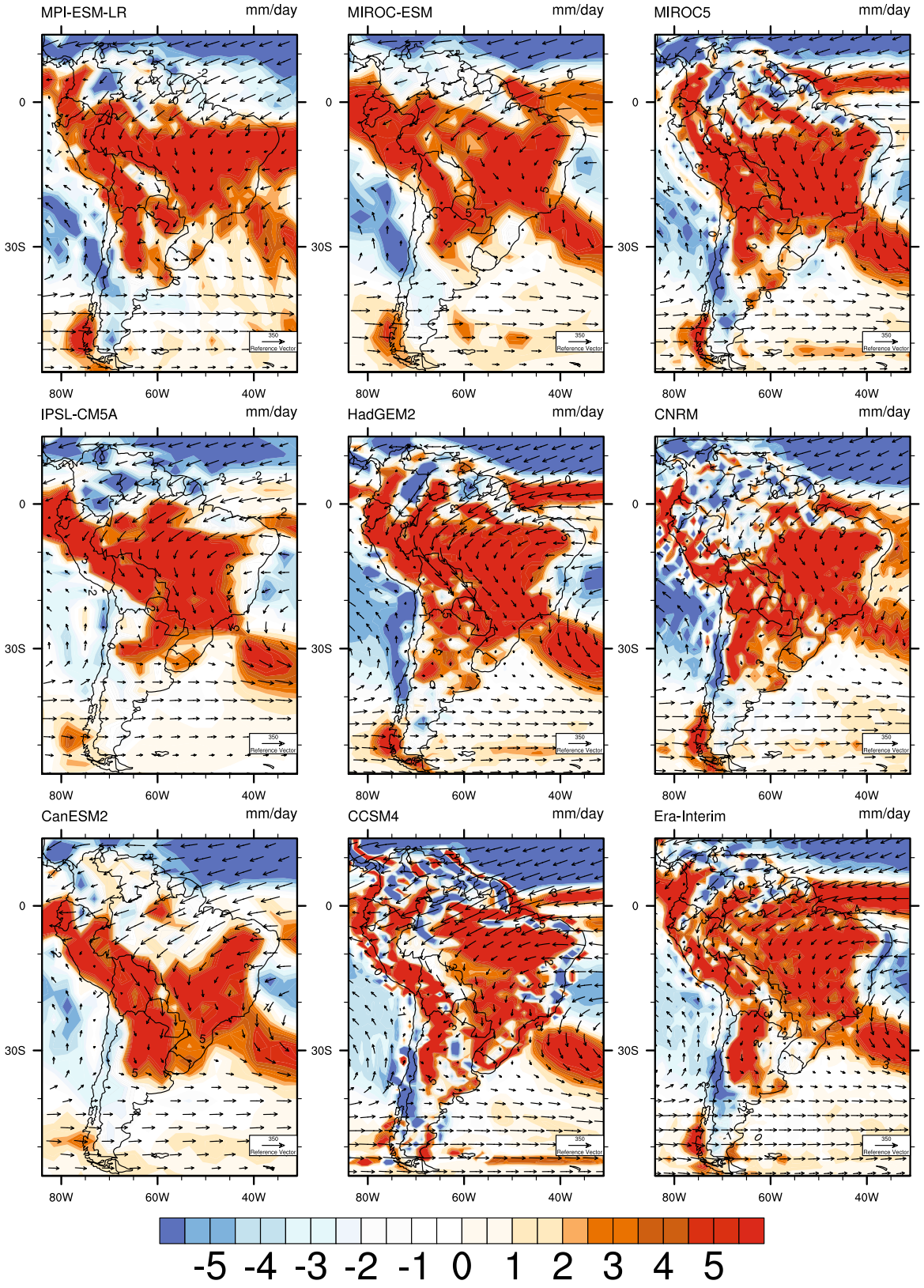

Fig. 10 Climatology (1979–2005) of vertically integrated moisture transport (vectors) in $kgm^{-1}s^{-1}$ and its convergence (contours) in mm/day in January (**a**) and July (**b**). The model data are shown at their original spatial resolution

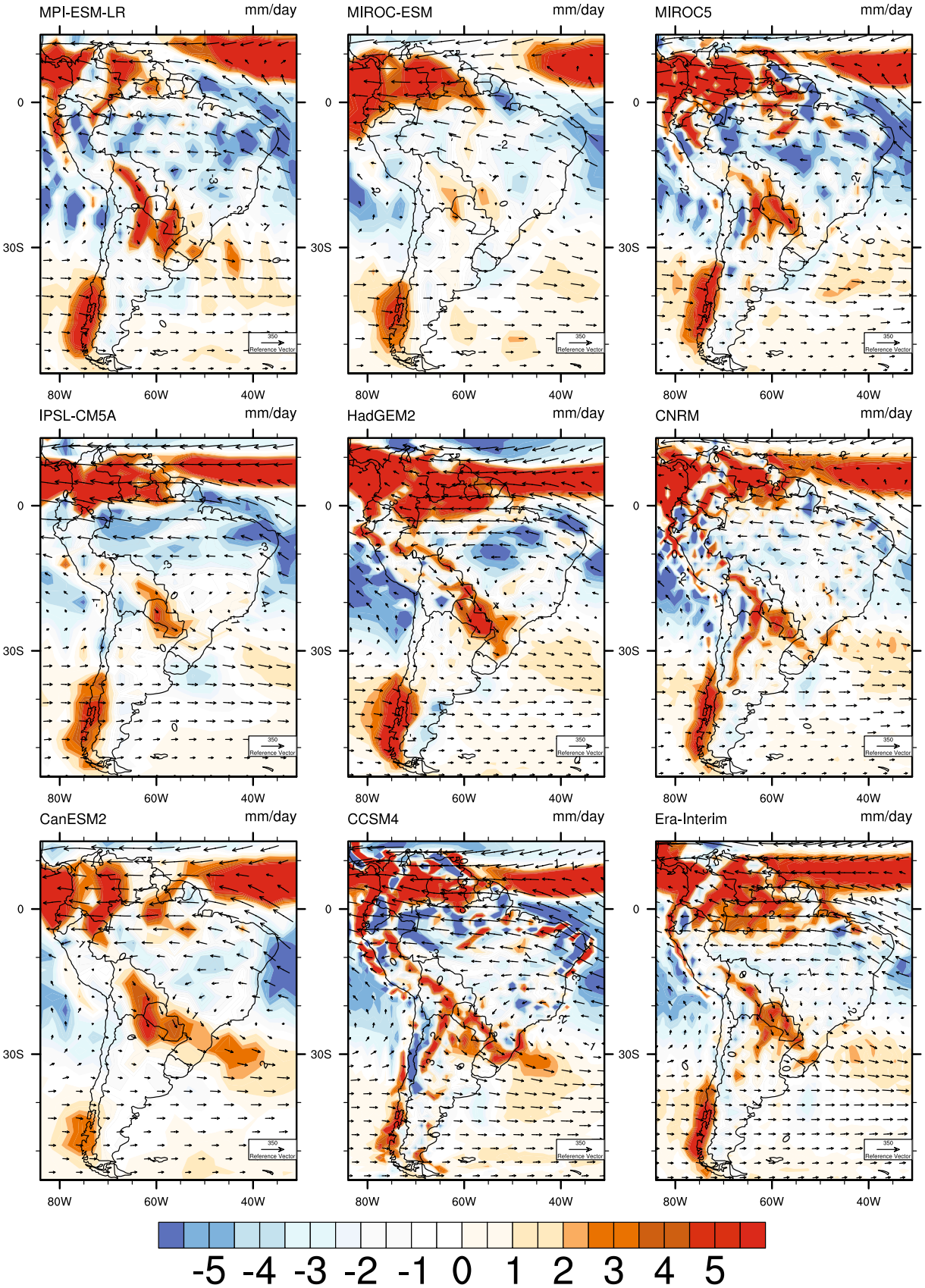

Fig. 10 (continued)

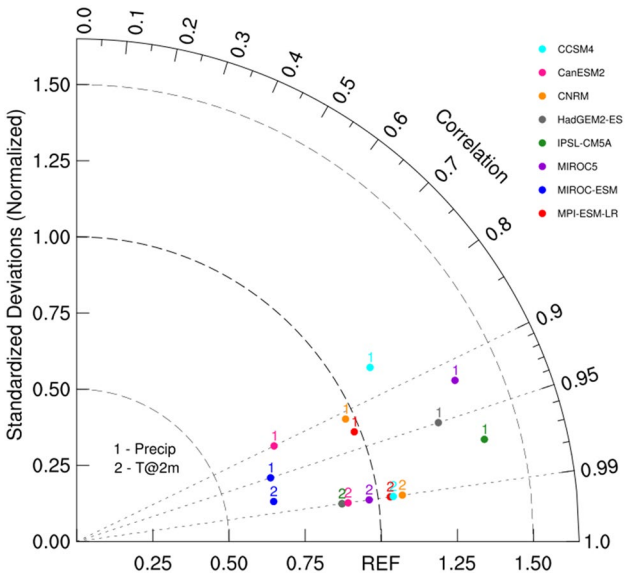

Fig. 11 Taylor diagram of the spatial pattern of January mean of precipitation and temperature for the eight CMIP5 models over Bolivia. The standard deviations have been normalized relative to the observed values. Each model is represented by a different color specified in the legend and numbers separate variables of precipitation and temperature. All models grids have been regridded to 2.5 degree for this analysis

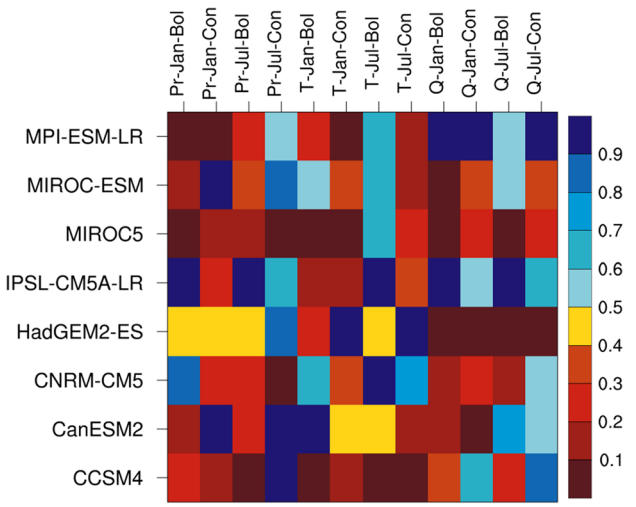

Fig. 12 Comparison of CMIP5 models across a set of continental (Con) and local (Bol; limited to Bolivia's boundaries) performance metrics based on bias values for precipitation (Pr), temperature (T) and vertically integrated moisture convergence (Q) for January and July. Biases are normalized relative to the range of bias values across models. Red shades represent lower relative bias values and blue shades show higher relative bias values

meaning a better (worse) performance of that model for that variable (Sheffield et al. 2013). We conclude that MPI-ESM-LR, MIROC5, CCSM4 are performing the best specifically for precipitation and temperature in the wet season and IPSL-CM5A-LR and HadGEME2-ES are doing the worst.

5 Summary

Bolivia is a country in South America with a historically small contribution to global greenhouse gas emissions. Yet the effects of climate change are already a reality for Bolivia. This study is the first phase of a more comprehensive project on climate change assessment on Bolivia. One source of uncertainty in possible future climate change is related to the parent GCMs used to drive high-resolution downscaling models. In this research, we evaluated historical simulations from eight CMIP5 GCMs, with the goal of selecting the three best available models in terms of their performance to provide large-scale forcing for dynamical downscaling. In this analysis, only the impact-related variables of surface temperature, precipitation, wind fields and moisture fluxes were investigated and compared against reanalysis datasets. Overall, the GCMs evaluated all perform reasonably well over South America at the large scale while regionally they differ.

Our major findings indicate that, in general, the selected CMIP5 GCMs have more difficulty simulating precipitation comparing to other analyzed variables, especially in the wet months of the summer. Finally, the primary aim of this study is to identify better performing GCMs in order to reduce the inherited biases in the downscaling process. Future work will focus on evaluating downscaled outputs from WRF for present-day climate and future climate change in Bolivia.

Acknowledgements This work was initially supported by the Ministry of Environment and Water (MMAyA) of the Plurinational State of Bolivia (contract MMAyA/PPCR no 117/2012 to RO and CR). We acknowledge further support from the Interamerican Development Bank (to RO and CR) for the development of tools and techniques used in this research, the Daugherty Water for Food Global Institute (post-doctoral support to RM), and the UNL Holland Computing Center. We also acknowledge the World Climate Research Programme's Working Group on Coupled Modelling, which is responsible for CMIP, and we thank the climate modeling groups (listed in Table 1 of this paper) for producing and making available their model output. For CMIP the U.S. Department of Energy's Program for Climate Model Diagnosis and Intercomparison provides coordinating support and led development of software infrastructure in partnership with the Global Organization for Earth System Science Portals.

References

Adler RF, Huffman GJ, Chang A et al (2003) The version-2 global precipitation climatology project (GPCP) monthly precipitation analysis(1979–Present). J Hydrometeorol 4:1147–1167. doi:10.1175/1525-7541(2003)004<1147:tvgpcp>2.0.co;2

Arora VK, Scinocca JF, Boer GJ et al (2011) Carbon emission limits required to satisfy future representative concentration pathways of greenhouse gases. Geophys Res Lett. doi:10.1029/2010gl046270

Arraut JM, Satyamurty P (2009) Precipitation and water vapor transport in the Southern Hemisphere with emphasis on the South American region. J Appl Meteorol Climatol 48(9):1902–1912. doi:10.1175/2009JAMC2030.1

Berbery EH, Barros VR (2002) The hydrologic cycle of the La Plata basin in South America. J Hydrometeorol 3:630–645. doi:10.1175/1525-7541(2002)003<0630:THCOTL>2.0.CO;2

Blacutt LA, Herdies DL, Gonçalves LGGD et al (2015) Precipitation comparison for the CFSR, MERRA, TRMM3B42 and combined scheme datasets in Bolivia. Atmos Res 163:117–131. doi:10.1016/j.atmosres.2015.02.002

Byerle LA, Paegle J (2002) Description of the seasonal cycle of low-level flows flanking the Andes and their interannual variability. 10th Conf Mt Meteorol MAP Meet 2002 27:71–88

Campetella CM, Vera CS (2002) The influence of the Andes mountains on the South American low-level flow. Geophys Res Lett 29(17):1826. doi:10.1029/2002GL015451

Carvalho LMV, Silva A, Jones C et al (2011) Moisture transport and intraseasonal variability in the South America monsoon system. Clim Dyn 36(9):1865–1880. doi:10.1007/s00382-010-0806-2

Chou SC, Marengo JA, Lyra AA et al (2011) Downscaling of South America present climate driven by 4-member HadCM3 runs. Clim Dyn 38:635–653. doi:10.1007/s00382-011-1002-8

Cook SJ, Kougkoulos I, Edwards LA et al (2016) Glacier change and glacial lake outburst flood risk in the Bolivian Andes. The Cryosphere 10:2399–2413. doi:10.5194/tc-10-2399-2016

Dee DP, Uppala SM, Simmons AJ et al (2011) The ERA-Interim reanalysis: configuration and performance of the data assimilation system. Q J R Meteor Soc 137:553–597. doi:10.1002/qj.828

Dufresne JL, Foujols MA, Denvil S et al (2013) Climate change projections using the IPSL-CM5 earth system model: from CMIP3 to CMIP5. Clim Dyn 40:2123–2165. doi:10.1007/s00382-012-1636-1

FAO (2010) Global forest resources assessment 2010. FAO forestry paper 163. ISBN 978-92-5-106654-6. http://www.fao.org/docrep/013/i1757e/i1757e.pdf

Gan MA, Kousky VE, Ropelewski CF (2004) The South America monsoon circulation and its relationship to rainfall over west-central Brazil. J Clim 17(1):47–66. doi:10.1175/1520-0442(2004)017<0047:TSAMCA>2.0.CO;2

Garreaud R, Vuille M, Clement AC (2003) The climate of the Altiplano: observed current conditions and mechanisms of past changes. Palaeogeogr, Palaeoclimatol Palaeoecol 194:5–22. doi:10.1016/S0031-0182(03)00269-4

Garreaud RCAD, Vuille M, Compagnucci R et al (2009) Present-day South American climate. Palaeogeogr Palaeoclimatol Palaeoecol 281:180–195. doi:10.1016/j.palaeo.2007.10.032

Gent PR, Danabasoglu G, Donner LJ et al (2011) The community climate system model version 4. J Clim 24:4973–4991. doi:10.1175/2011jcli4083.1

Gleckler PJ, Taylor KE, Doutriaux C (2008) Performance metrics for climate models. J Geophys Res. doi:10.1029/2007jd008972

Grau HR, Aide M (2008) Globalization and land-use transitions in Latin America. Ecol Soc. doi:10.5751/es-02559-130216

Grimm AM (2011) Interannual climate variability in South America: impacts on seasonal precipitation, extreme events, and possible effects of climate change. Stoch Env Res Risk A 25(4):537–554. 10.1007/s00477-010-0420-1

Haylock MR, Peterson TC, Alves LM et al (2006) Trends in total and extreme South American rainfall in 1960–2000 and links with sea surface temperature. J Clim 19(8):1490–1512. doi:10.1175/JCLI3695.1

Insel N, Poulsen CJ, Sturm C et al (2013) Climate controls on Andean precipitation δ18O interannual variability. J Geophys Res Atmos 118:9721–9742. doi:10.1002/jgrd.50619

IPCC (2013) Climate change 2013: the physical science basis. In: Stocker TF, Qin D, Plattner GK, Tignor M, Allen SK, Boschung J, Nauels A, Xia Y, Bex V, Midgley PM (eds) Contribution of working group I to the fifth assessment report of the intergovernmental panel on climate change. Cambridge University Press, Cambridge

Jones C, Carvalho LMV (2013) Climate change in the South American monsoon system: present climate and CMIP5 projections. J Clim 26:6660–6678. doi:10.1175/jcli-d-12-00412.1

Jones CD, Hughes JK, Bellouin N et al (2011) The HadGEM2-ES implementation of CMIP5 centennial simulations. Geosci Model Dev 4:543–570. doi:10.5194/gmd-4-543-2011

Lenters JD, Cook KH (1997) On the origin of the Bolivian high and related circulation features of the South American climate. J Atmos Sci 54:656–678. doi:10.1175/1520-0469(1997)054<0656:otootb>2.0.co;2

Lenters JD, Cook KH (1999) Summertime precipitation variability over South America: role of the large-scale circulation. Mon Weather Rev 127:409–431. doi:10.1175/1520-0493(1999)127<0409:spvosa>2.0.co;2

Liebmann B, Mechoso CR (2011) The South American monsoon system. Glob Monsoon Syst World Sci Ser Asia Pac Weather Clim. doi:10.1142/9789814343411_0009

Liebmann B, Kiladis GN, Vera CS et al (2004) Subseasonal variations of rainfall in South America in the vicinity of the low-level jet east of the Andes and comparison to those in the South Atlantic convergence zone. J Clim 17(19):3829–3842. doi:10.1175/1520-0442(2004)017<3829:SVORIS>2.0.CO;2

Marengo JA, Soares WR, Saulo C et al (2004) Climatology of the low-level jet east of the Andes as derived from the NCEP-NCAR reanalyses: characteristics and temporal variability. J Clim 17(12):2261–2280. doi:10.1175/1520-0442(2004)017<2261:cotlje>2.0.co;2

Marengo JA, Liebmann B, Grimm AM et al (2012) Recent developments on the South American monsoon system. Int J Clim. doi:10.1002/joc.2254

Marengo JA, Chou SC, Torres RR et al A (2014) Climate change in Central and South America: recent trends, future projections, and impacts on regional agriculture. CGIAR Res Progr Clim Change, Agric Food Secur (CCAFS) 73:93

Newman M, Kiladis GN, Weickmann KM et al (2012) Relative contributions of synoptic and low-frequency eddies to time-mean atmospheric moisture transport, including the role of atmospheric rivers. J Clim 25:7341–7361. doi:10.1175/jcli-d-11-00665.1

Nogués-Paegle J, Mechoso CR, Fu R et al (2002) Progress in Pan American CLIVAR research: understanding the South American monsoon. Meteorologica 27:1–30

Oglesby R, Rowe C, Grunwaldt A et al (2016) A high-resolution modeling strategy to assess impacts of climate change for Mesoamerica and the Caribbean. Am J Clim Change 05:202–228. doi:10.4236/ajcc.2016.52019

Ovando A, Tomasella J, Rodriguez DA et al (2016) Extreme flood events in the Bolivian Amazon wetlands. J Hydrol Reg Stud 5:25. doi:10.1016/j.ejrh.2016.01.024

Penven P (2005) Average circulation, seasonal cycle, and mesoscale dynamics of the Peru current system: a modeling approach. J Geophys Res. doi:10.1029/2005jc002945

Raia A, Cavalcanti IFA (2008) The life cycle of the South American monsoon system. J Clim 21(23):6227–6246. doi:10.1175/2008JCLI2249.1

Rupp DE, Abatzoglou JT, Hegewisch KC et al (2013) Evaluation of CMIP5 20th century climate simulations for the Pacific Northwest USA. J Geophys Res Atmos. doi:10.1002/jgrd.50843

Salazar A, Baldi G, Hirota M et al (2015) Land use and land cover change impacts on the regional climate of non-Amazonian South America: a review. Glob Planet Change. doi:10.1016/j.gloplacha.2015.02.009

Salio P, Nicolini M, Zipser EJ (2007) Mesoscale convective systems over southeastern South America and their relationship with the South American low-level jet. Mon Weather Rev 135:1290–1309. doi:10.1175/mwr3305.1

Sánchez-Azofeifa GA, Portillo-Quintero C (2011) Extent and drivers of change of neotropical seasonally dry tropical forests. Seas Dry Trop For. doi:10.5822/978-1-61091-021-7_3

Satyamurty P, Wanzeler da Costa CP, Manzi AO (2013) Moisture source for the Amazon Basin: a study of contrasting years. Theor Appl Climatol 111(1–2):195–209. doi:10.1007/s00704-012-0637-7

Seiler C, Hutjes RWA, Kabat P (2013a) Climate variability and trends in Bolivia. J Appl Meteorol Climatol 52:130–146. doi:10.1175/jamc-d-12-0105.1

Seiler C, Hutjes RWA, Kabat P (2013b) Likely ranges of climate change in Bolivia. J Appl Meteorol Climatol 52:1303–1317. doi:10.1175/jamc-d-12-0224.1

Sheffield J, Barrett AP, Colle B et al (2013) North American climate in CMIP5 experiments. Part I: evaluation of historical simulations of continental and regional climatology*. J Clim 26:9209–9245. doi:10.1175/jcli-d-12-00592.1

Soares WR, Marengo JA (2009) Assessments of moisture fluxes east of the Andes in South America in a global warming scenario. Int J Clim 29:1395–1414. doi:10.1002/joc.1800

Solman SA, Sanchez E, Samuelsson P et al (2013) Evaluation of an ensemble of regional climate model simulations over South America driven by the ERA-Interim reanalysis: model performance and uncertainties. Clim Dyn 41(5–6):1139–1157. 10.1007/s00382-013-1667-2

Taylor KE, Stouffer RJ, Meehl GA (2012) An overview of CMIP5 and the experiment design. Bull Am Meteor Soc 93:485–498. doi:10.1175/bams-d-11-00094.1

Trenberth KE, Fasullo JT, Mackaro J (2011) Atmospheric moisture transports from ocean to land and global energy flows in reanalyses. J Clim 24:4907–4924. doi:10.1175/2011jcli4171.1

Vera CS, Vigliarolo PK, Berbery EH (2002) Cold season synoptic-scale waves over subtropical South America. Mon Weather Rev 130(3):684–699. doi:10.1175/1520-0493(2002)130<0684:CSSSWO>2.0.CO;2

Vera C, Silvestri G, Liebmann B, González P (2006a) Climate change scenarios for seasonal precipitation in South America from IPCC-AR4 models. Geophys Res Lett. doi:10.1029/2006gl025759

Vera C, Baez J, Douglas M et al (2006b) The South American low-level jet experiment. Bull Am Meteor Soc 87:63–77. doi:10.1175/bams-87-1-63

Vicente-Serrano SM, Chura O, López-Moreno JI et al (2014) Spatio-temporal variability of droughts in Bolivia: 1955–2012. Int J Clim 35:3024–3040. doi:10.1002/joc.4190

Voldoire A, Sanchez-Gomez E, Mélia DSY et al (2012) The CNRM-CM5.1 global climate model: description and basic evaluation. Clim Dyn 40:2091–2121. doi:10.1007/s00382-011-1259-y

Wanzeler da Costa CP, Satyamurty P (2016) Inter-hemispheric and inter-zonal moisture transports and monsoon regimes. Int J Clim 36(15):4705–4722. doi:10.1002/joc.4662

Watanabe M, Suzuki T, O'Ishi R et al (2010) Improved climate simulation by MIROC5: mean states, variability, and climate sensitivity. J Clim 23:6312–6335. doi:10.1175/2010jcli3679.1

Watanabe S, Hajima T, Sudo K et al (2011) MIROC-ESM: model description and basic results of CMIP5-20c3m experiments. Geosci Model Dev Discuss 4:1063–1128. doi:10.5194/gmdd-4-1063-2011

Wheeler D (2011) Quantifying vulnerability to climate change: implications for adaptation assistance. SSRN Electron J. doi:10.2139/ssrn.1824611

Zanchettin D, Rubino A, Matei D et al (2012) Multidecadal-to-centennial SST variability in the MPI-ESM simulation ensemble for the last millennium. Clim Dyn 40:1301–1318. doi:10.1007/s00382-012-1361-9

Zhou J, Lau KM (1998) Does a monsoon climate exist over South America? J Clim 11(5):1020–1040. doi:10.1175/1520-0442(1998)011<1020:DAMCEO>2.0.CO;2

Zhou J, Lau KM (2001) Principal modes of interannual and decadal variability of summer rainfall over South America. Int J Clim 21(13):1623–1644. doi:10.1002/joc.700